

Three-Coordinate Copper(II) Alkynyl Complex in C–C Bond Formation: The Sesquicentennial of the Glaser Coupling

Abolghasem Bakhoda,[‡] Otome E. Okoromoba,[‡] Christine Greene, Mahdi Raghibi Boroujeni, Jeffery A. Bertke, and Timothy H. Warren*



Cite This: *J. Am. Chem. Soc.* 2020, 142, 18483–18490



Read Online

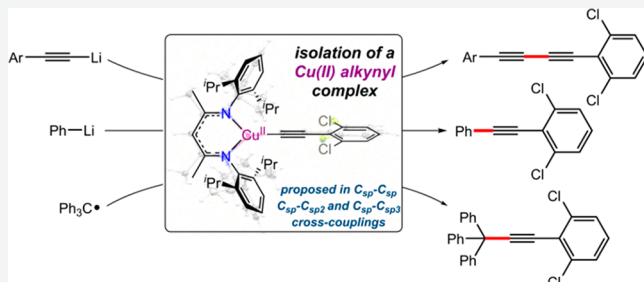
ACCESS |

Metrics & More

Article Recommendations

Supporting Information

ABSTRACT: Copper(II) alkynyl species are proposed as key intermediates in numerous Cu-catalyzed C–C coupling reactions. Supported by a β -diketiminate ligand, the three-coordinate copper(II) alkynyl $[\text{Cu}^{\text{II}}]-\text{C}\equiv\text{CAr}$ ($\text{Ar} = 2,6\text{-Cl}_2\text{C}_6\text{H}_3$) forms upon reaction of the alkyne $\text{H}-\text{C}\equiv\text{CAr}$ with the copper(II) *tert*-butoxide complex $[\text{Cu}^{\text{II}}]-\text{O}^{\prime}\text{Bu}$. In solution, this $[\text{Cu}^{\text{II}}]-\text{C}\equiv\text{CAr}$ species cleanly transforms to the Glaser coupling product $\text{ArC}\equiv\text{C}-\text{C}\equiv\text{CAr}$ and $[\text{Cu}^{\text{I}}](\text{solvent})$. Addition of nucleophiles $\text{R}'\text{C}\equiv\text{C}-\text{Li}$ ($\text{R}' = \text{aryl, silyl}$) and $\text{Ph}-\text{Li}$ to $[\text{Cu}^{\text{II}}]-\text{C}\equiv\text{CAr}$ affords the corresponding $\text{C}_{\text{sp}}-\text{C}_{\text{sp}}$ and $\text{C}_{\text{sp}}-\text{C}_{\text{sp}2}$ coupled products $\text{RC}\equiv\text{C}-\text{C}\equiv\text{CAr}$ and $\text{Ph}-\text{C}\equiv\text{CAr}$ with concomitant generation of $[\text{Cu}^{\text{I}}](\text{solvent})$ and $\{[\text{Cu}^{\text{I}}]-\text{C}\equiv\text{CAr}\}^-$, respectively. Supported by density functional theory (DFT) calculations, redox disproportionation forms $[\text{Cu}^{\text{III}}](\text{C}\equiv\text{CAr})(\text{R})$ species that reductively eliminate $\text{R}-\text{C}\equiv\text{CAr}$ products. $[\text{Cu}^{\text{II}}]-\text{C}\equiv\text{CAr}$ also captures the trityl radical $\text{Ph}_3\text{C}\cdot$ to give $\text{Ph}_3\text{C}-\text{C}\equiv\text{CAr}$. Radical capture represents the key $\text{C}_{\text{sp}}-\text{C}_{\text{sp}3}$ bond-forming step in the copper-catalyzed C–H functionalization of benzylic substrates $\text{R}-\text{H}$ with alkynes $\text{H}-\text{C}\equiv\text{CR}'$ ($\text{R}' = (\text{hetero})\text{aryl, silyl}$) that provide $\text{C}_{\text{sp}}-\text{C}_{\text{sp}3}$ coupled products $\text{R}-\text{C}\equiv\text{CR}$ via radical relay with $^{\prime}\text{BuOO}^{\prime}\text{Bu}$ as oxidant.



INTRODUCTION

Transition metal-mediated carbon–carbon bond formation represents one of the most fundamental transformations in chemical and material synthesis.¹ Carl Glaser developed the first copper-mediated oxidative coupling of terminal alkynes 150 years ago, suggesting copper organometallic intermediates in the $\text{C}_{\text{sp}}-\text{C}_{\text{sp}}$ coupling of phenylacetylene ($\text{H}-\text{C}\equiv\text{C}-\text{Ph}$) to give the diyne $\text{Ph}-\text{C}\equiv\text{C}-\text{C}\equiv\text{C}-\text{Ph}$ via reaction of ammoniacal cuprous chloride with oxygen as the oxidant (Figure 1a).² Glaser suggested that copper(I) acetylide dimer forms and undergoes oxidation by O_2 to ultimately release $\text{Ph}-\text{C}\equiv\text{C}-\text{C}\equiv\text{C}-\text{Ph}$.²

A number of mechanistic proposals have evolved to explain the Glaser $\text{C}_{\text{sp}}-\text{C}_{\text{sp}}$ coupling (Figure 1a). Salkind and Fundyler offered an early proposition that involved alkyne deprotonation followed by oxidation via copper(II) to form an alkynyl radical that dimerizes to give the 1,3-diyne product (Figure 2a).³ On the basis of a combination of kinetic studies and the prevalence of selective homocoupling in mixtures of alkynes, Bohlman discounted a radical mechanism and put forth dimeric copper(II) acetylides as key species in C–C coupling (Figure 2b).⁴ As part of a detailed mechanistic study of the Glaser–Hay reaction, which enables catalytic dimerization of terminal alkynes with O_2 as a terminal oxidant, Vilhelmsen, Nielsen, and co-workers suggested a new role for a discrete copper(II) acetylide complex (Figure 2c).^{5,6} They proposed that a

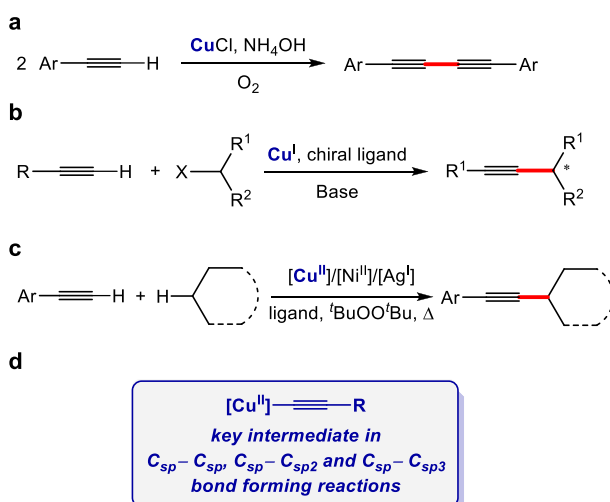
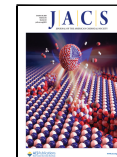


Figure 1. Proposed Cu alkynyl intermediates in $\text{C}_{\text{sp}}-\text{C}_{\text{sp}}$, $\text{C}_{\text{sp}}-\text{C}_{\text{sp}2}$, and $\text{C}_{\text{sp}}-\text{C}_{\text{sp}3}$ bond-forming reactions.

Received: July 2, 2020

Published: September 21, 2020



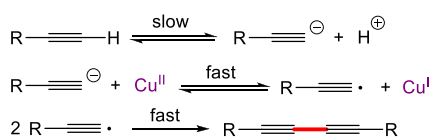
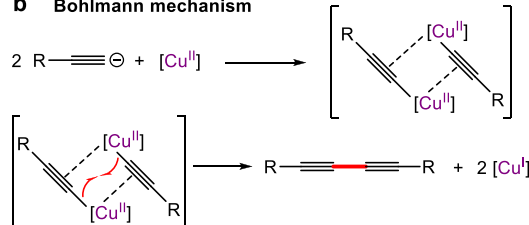
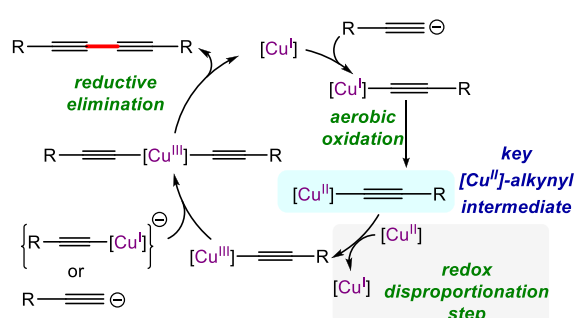
a Salkind and Fundyler mechanism**b** Bohlmann mechanism**c** Nielsen and Vilhelmsen mechanism

Figure 2. Mechanistic proposals for copper(II)-promoted $C_{sp}-C_{sp}$ coupling. (a) Homocoupling of alkynyl radicals (Salkind and Fundyler). (b) Dimerization of Cu^{II} alkynyl intermediates (Bohlmann). (c) Redox disproportionation of Cu^{II} acetylide to $[Cu^{III}](C\equiv CR)_2$ intermediate that undergoes C–C reductive coupling (Nielsen and Vilhelmsen).

copper(I) acetylide (formed upon deprotonation of the alkyne in the presence of a copper(I) source)⁷ is aerobically oxidized to the corresponding copper(II) acetylide.⁵ Redox disproportionation of this copper(II) acetylide generates a cationic copper(III) acetylide and a nucleophilic copper(I) acetylide that can combine to give a copper(III) bis(acetylide) species that is susceptible to reductive elimination to give the C–C coupled 1,3-diyne product.

Such copper(II) alkynyl intermediates are also envisioned in several copper-catalyzed organic transformations such as oxidative $C_{sp}-C_{sp}$ couplings (Figure 1b), trifluoromethylalkynylation of alkenes, [3 + 2] cycloaddition with azides, oxidative $C_{sp^3}-H/C_{sp}-H$ cross-couplings (Figure 1c), oxidative coupling of terminal alkynes, deacetylation coupling of yrones, and oxidative amidation of terminal alkynes.^{8–19} For instance, recent Pd-free Sonogashira-type reactions that form $C_{sp}-C_{sp^3}$ or $C_{sp}-C_{sp^2}$ bonds have been proposed to proceed through the intermediacy of a copper(II) alkynyl species.^{8,20,21} Such cupric acetylides were also proposed by Liu and co-workers as intermediates in the enantioselective trifluoromethylalkynylation of alkenes under particularly mild conditions.⁹ Recently, Lei and co-workers reported the cross-dehydrogenative coupling of terminal alkynes with unactivated alkanes using a multimetal-catalyzed reaction strategy to prepare internal alkynes (Figure 1c) that was also proposed to proceed via copper(II) alkynyl intermediates.^{11–14} Most recently, Liu and

his team reported an elegant methodology for the enantioselective alkynylation of benzylic C–H bonds via a radical relay mechanism. Employing *N*-fluorodi(benzenesulfonyl)amine (NFSI) as an oxidant, they proposed chiral (bisoxazoline) Cu^{II} alkynyl species as key intermediates that enantioselectively capture benzylic radicals.¹⁹

Despite numerous examples of well-characterized copper(I) acetylides complexes,²² copper(II) alkynyls, and in general any structurally well-defined organocopper(II) complexes, are extremely rare.²³ In 2017, Tilley and co-workers described the mixed-valent $Cu(I)Cu(II) \mu$ -alkynyl complex $\{[DPFN]_2Cu(\mu-\eta^1:\eta^1-C\equiv CAR-Me)\}^{2+}$ ($DPFN = 2,7$ -bis[fluorodi(2-pyridyl)methyl]-1,8-naphthyridine; $Arp-Me = 4$ -MeC₆H₄) as stable toward diyne formation (Figure 3a).²⁴ Inspired by a β -diketiminato mononuclear copper(II) aryl complex isolated in our laboratory (Figure 3b),²⁵ we targeted a discrete, mononuclear copper(II) alkynyl $[Cu^{II}]-C\equiv CAr$.

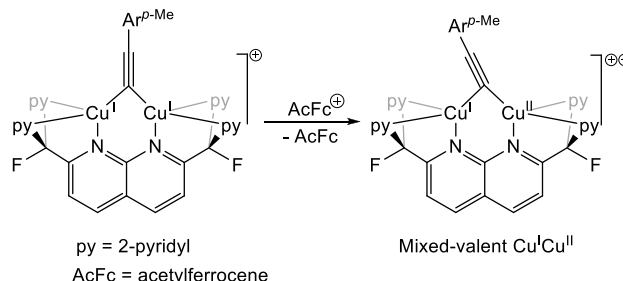
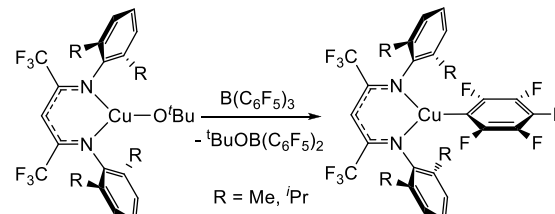
a Mixed-valent $Cu_2(I,II) \mu$ -alkynyl complex by Tilley and coworkers**b** Three-coordinate $Cu(II)$ aryl complex by Warren and coworkers

Figure 3. Structurally well-defined organocopper(II) compounds.

RESULTS AND DISCUSSION

Synthesis, Characterization, and Reactivity of a Copper(II) Alkynyl Complex. Reaction of the copper(I) β -diketiminato complex $[^3Pr_2NN]Cu(NCMe)$ ²⁶ (1-MeCN) with $^3BuOO^3Bu$ at room temperature (RT) gives $[^3Pr_2NN]Cu^{II}-O^3Bu$ (2). This three-coordinate Cu(II) alkoxide is similar in structure to several related $[Cu^{II}]-O^3Bu$ species (Figure S20) and possesses closely related spectroscopic parameters.^{27–29} Addition of $H-C\equiv CAr^{Cl2}$ ($Ar^{Cl2} = 2,6-Cl_2C_6H_3$) to 2 in *n*-pentane at RT results in a color change from brown to dark violet. The choice of the terminal alkyne was crucial in order to successfully synthesize and isolate the terminal, three-coordinate copper(II) alkynyl complex. While the reaction of a range of alkyl- and arylacetylenes $H-C\equiv CR$ and $H-C\equiv CAr$ were examined with $[^3Pr_2NN]Cu^{II}-O^3Bu$ (2), ultimately 2,6-dichlorophenylacetylene $H-C\equiv CAr^{Cl2}$ possessed an appropriate combination of steric protection and C–H acidity to cleanly furnish the terminal Cu(II) alkynyl 3. Crystallization from *n*-pentane affords dark violet crystals of $[^3Pr_2NN]Cu-C\equiv CAr^{Cl2}$ (3) in 41% isolated yield (Figure 4a). The X-ray

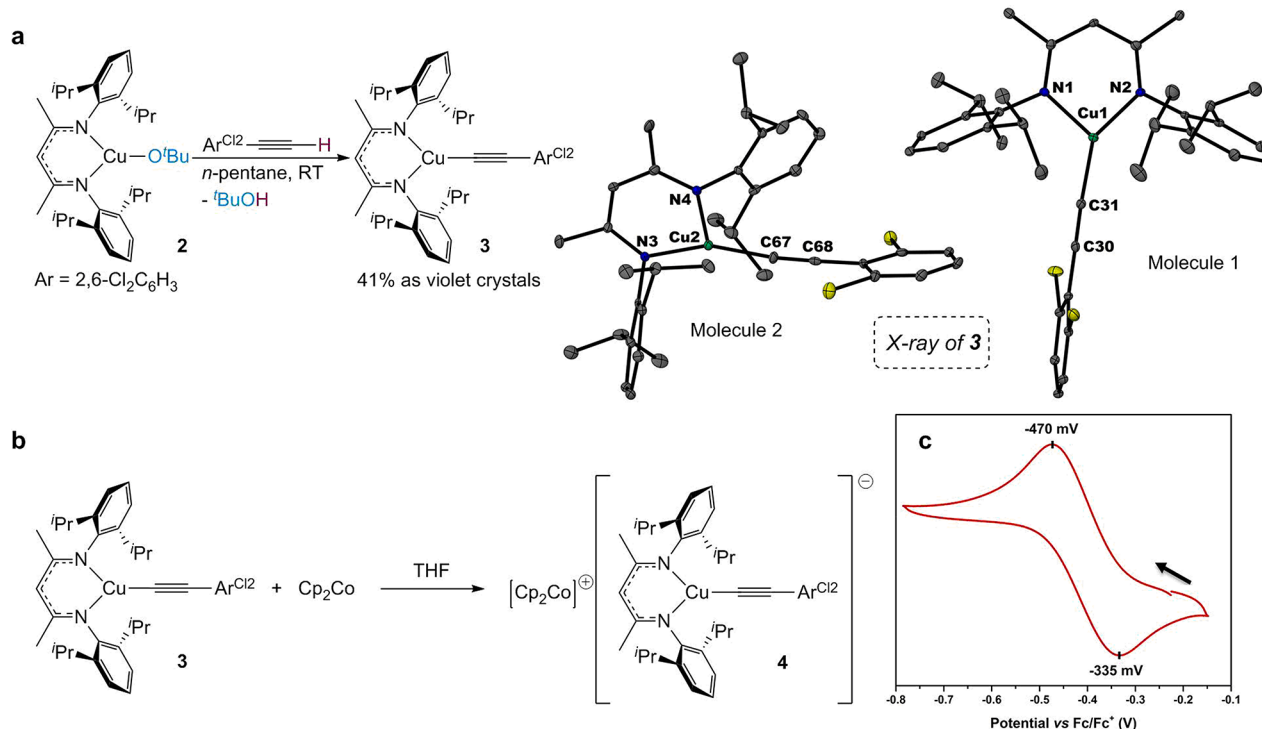


Figure 4. Synthesis and isolation of the three-coordinate Cu(II) alkynyl 3. (a) Synthesis and X-ray crystal structure of $[\text{iPr}_2\text{NN}]^+ \text{Cu}-\text{C}\equiv\text{CAr}^{\text{Cl}2}$ (3). (b) One-electron reduction of 3 with cobaltocene to generate $[\text{Cp}_2\text{Co}]^+ \{[\text{iPr}_2\text{NN}]^+ \text{Cu}-\text{C}\equiv\text{CAr}^{\text{Cl}2}\}^-$ ($\text{Cp}_2\text{Co}^+ \cdot 4$). (c) Cyclic voltammogram at 20 mV/s of 3 in fluorobenzene (1.8 mM) at 23 °C with 0.1 M $\text{NaBAr}_4^{\text{F}}$ ($\text{Ar}^{\text{F}} = 3,5-(\text{CF}_3)_2\text{C}_6\text{H}_3$) as a supporting electrolyte.

structure of 3 reveals two nearly identical, yet crystallographically independent, molecules featuring trigonal planar coordination at the Cu centers (Σ (angles about Cu) = 359.72(7) and 359.60(8)°). The Cu–C_{alkynyl} distances of 1.887(5) and 1.872(6) Å are on the low end of those reported for Cu(I) acetylides (1.87–1.98 Å).²² The large disparity of the two N–Cu–C angles in 3 (molecule 1, 142.5(2) and 122.0(2)°; molecule 2, 150.6(2) and 112.9(2)°) and the shortened Cu–N distance distal to the Cu–C unit (Cu–N distances: molecule 1, 1.907(4) and 1.859(4) Å; molecule 2, 1.903(4) and 1.861(4) Å) result in a Y-shaped geometry around the Cu atom. In the solid state there is a π -stacking interaction between an electron-rich N-aryl ring of molecule 1 and an electron-deficient alkynyl dichlorophenyl ring of molecule 2 (Figure 4a).

The isotropic X-band electron paramagnetic resonance (EPR) spectrum of 3 in toluene at 200 K shows a four-line signal characteristic of a mononuclear Cu(II) center (Figure S5). Simulation of the isotropic EPR spectrum provides $g_{\text{iso}} = 2.097$ with $A_{\text{iso}}(\text{Cu}) = 210$ and $A_{\text{iso}}(\text{N}) = 40$ MHz. The frozen glass EPR spectrum of 3 in toluene at 80 K is axially biased with $g_1 = 2.178$, $g_2 = 2.040$, and $g_3 = 2.050$ with $A_1(\text{Cu}) = 130$, $A_2(\text{Cu}) = 290$, and $A_3(\text{Cu}) = 130$ MHz, respectively (Figure S6). These data are in good agreement with previously reported axially biased three-coordinate $[\text{Cu}^{\text{II}}]-\text{X}$ species (X = amide, alkoxide, thiolate, and halide) with $g_1 \approx 2.20$ and $g_{2,3} \approx 2.05$.^{27–32} The IR spectrum of 3 exhibits $\nu_{\text{C}\equiv\text{C}}$ at 2187 cm⁻¹ (Figure S7), while the optical spectrum of 3 in toluene shows a strong band at $\lambda_{\text{max}} = 580$ nm (4300 M⁻¹ cm⁻¹) (Figure S4).

Cyclic voltammetry of $[\text{iPr}_2\text{NN}]^+ \text{Cu}-\text{C}\equiv\text{CAr}^{\text{Cl}2}$ (3) in fluorobenzene (PhF) at RT exhibits a quasi-reversible reduction wave centered at -470 mV vs Fc^+/Fc (Figure 4c). Encouraged by this observation, reduction of 3 by cobaltocene

(Cp_2Co) in C_6D_6 at RT allows for in situ formation of the corresponding copper(I) acetylide $[\text{Cp}_2\text{Co}]^+ \{[\text{iPr}_2\text{NN}]^+ \text{Cu}-\text{C}\equiv\text{CAr}^{\text{Cl}2}\}^-$ ($\text{Cp}_2\text{Co}^+ \cdot 4$) as shown in Figure 4b. Unfortunately, this species decays in solution over a matter of minutes to form an insoluble yellow solid preventing characterization by X-ray crystallography. Nonetheless, ¹H NMR analysis of the reaction mixture in $\text{THF}-d_8$ (tetrahydrofuran) fully supports the diamagnetic nature of anionic $\text{Cp}_2\text{Co}^+ \cdot 4$. These spectroscopic signatures include a sharp, distinct doublet at δ 6.60 ppm and a triplet at δ 6.17 ppm that represents *meta*-H and *para*-H resonances of the $\text{Ar}^{\text{Cl}2}$ ring on the acetylide ligand, respectively, along with a diagnostic signal for the β -diketiminate backbone C–H methine at δ 4.75 ppm (Figure S9).

Mechanism for $\text{C}_{\text{sp}}-\text{C}_{\text{sp}}$ and $\text{C}_{\text{sp}}-\text{C}_{\text{sp}2}$ Coupling via $[\text{iPr}_2\text{NN}]^+ \text{Cu}-\text{C}\equiv\text{CAr}^{\text{Cl}2}$: **Experiment and Theory.** The copper(II) alkynyl $[\text{iPr}_2\text{NN}]^+ \text{Cu}-\text{C}\equiv\text{CAr}^{\text{Cl}2}$ (3) is unstable in solution at RT, transforming to $^{\text{Cl}2}\text{ArC}\equiv\text{C}-\text{C}\equiv\text{CAr}^{\text{Cl}2}$ (5) and $[\text{iPr}_2\text{NN}]^+ \text{Cu}(\text{solvent})$ over hours to minutes, depending on the solvent (Figure 5a). Surprisingly, the use of polar solvents such as MeCN accelerates diyne formation from $[\text{iPr}_2\text{NN}]^+ \text{Cu}-\text{C}\equiv\text{CAr}^{\text{Cl}2}$ (3) to form $^{\text{Cl}2}\text{ArC}\equiv\text{C}-\text{C}\equiv\text{CAr}^{\text{Cl}2}$ and $[\text{Cu}^{\text{II}}]-\text{NCMe}$ (1-MeCN) in 88% and 98% yields, respectively, within 5 min (Figure 5a). These observations run counter to the Bohlmann mechanism⁴ (Figure 2b), which requires a bimolecular interaction between $[\text{Cu}^{\text{II}}]-\text{C}\equiv\text{CR}$ species to form a less-polar dimer $\{[\text{Cu}^{\text{II}}]_2(\mu-\text{C}\equiv\text{CR})_2\}$. Moreover, a spontaneous loss of the $\cdot\text{C}\equiv\text{CAr}^{\text{Cl}2}$ radical from $[\text{Cu}^{\text{II}}]-\text{C}\equiv\text{CAr}^{\text{Cl}2}$ (3) connected to the Salkind and Fundyler mechanism³ (Figure 2a) is unlikely due to the high bond-dissociation free energy (BDFE) of the copper(II) acetylide bond calculated at 73.1 kcal/mol (BP86+GD₃BJ/6-311+G(d,p)/SMD-acetonitrile//BP86/6-311+G(d)/gas).

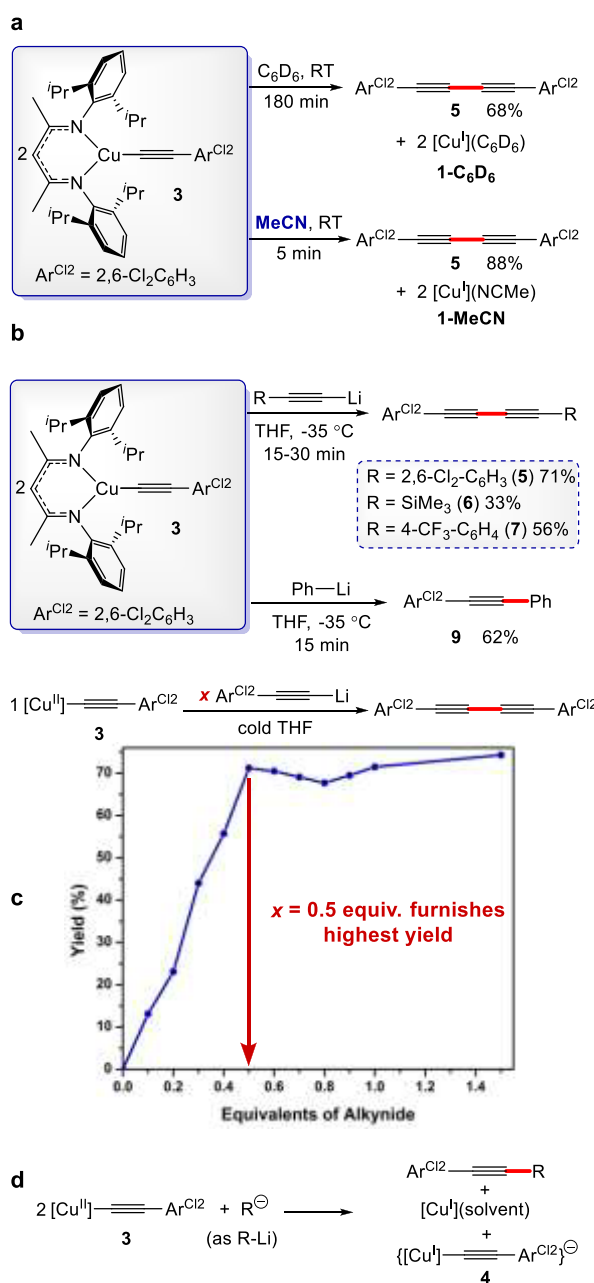


Figure 5. Mechanistic studies of Cu(II) alkynyl-mediated C–C coupling reactions. (a) $\text{C}_{\text{sp}}-\text{C}_{\text{sp}}$ and $\text{C}_{\text{sp}}-\text{C}_{\text{sp}2}$ coupling promoted by polar solvents (MeCN) or (b) organolithium nucleophiles ($\text{R}-\text{Li}$) mediated by Cu(II) alkynyl complex 3. (c) Yield of diyne 5 vs equivalents of $\text{Li}-\text{C}\equiv\text{C}\text{Ar}^{\text{Cl}2}$ added to 3, reaching a maximum yield with a $2[\text{Cu}^{\text{II}}]-\text{C}\equiv\text{C}\text{Ar}^{\text{Cl}2}:1\text{Li}-\text{C}\equiv\text{C}\text{Ar}^{\text{Cl}2}$ stoichiometry.

On the other hand, the addition of alkynide and phenyl nucleophiles R^- (as $\text{Li}-\text{R}$ reagents) to $[\text{Pr}_2\text{NN}]\text{Cu}-\text{C}\equiv\text{C}\text{Ar}^{\text{Cl}2}$ (3) spontaneously leads to $\text{R}-\text{C}\equiv\text{C}\text{Ar}^{\text{Cl}2}$ products according to the stoichiometry $2[\text{Cu}^{\text{II}}]-\text{C}\equiv\text{C}\text{Ar}^{\text{Cl}2}:1\text{Li}-\text{R}$ (Figure 5b). Addition of 1 equiv of $\text{Li}-\text{C}\equiv\text{C}\text{Ar}^{\text{Cl}2}$ ($\text{Ar}^{\text{Cl}2} = 2,6\text{-Cl}_2\text{C}_6\text{H}_3$) to 2 equiv of 3 in THF at -35°C provides the symmetric diyne $^{\text{Cl}2}\text{ArC}\equiv\text{C}-\text{C}\equiv\text{C}\text{Ar}^{\text{Cl}2}$ (5) in 71% yield (Figure 5b). Interestingly, the addition of 1 equiv of $\text{Li}-\text{C}\equiv\text{C}\text{Ar}^{\text{CF}3}$ ($\text{Ar}^{\text{CF}3} = 4\text{-CF}_3\text{C}_6\text{H}_4$) to 2 equiv of 3 in cold THF results in an immediate color change from violet to bright orange and formation of the

corresponding unsymmetric 1,3-diyne $\text{TMS}-\text{C}\equiv\text{C}-\text{C}\equiv\text{C}\text{Ar}^{\text{Cl}2}$ (6) or $^{\text{CF}3}\text{ArC}\equiv\text{C}-\text{C}\equiv\text{C}\text{Ar}^{\text{Cl}2}$ (7) in 33% and 56% yields, respectively (Figure 5b). In each case, the homocoupled 1,3-diyne $^{\text{Cl}2}\text{ArC}\equiv\text{C}-\text{C}\equiv\text{C}\text{Ar}^{\text{Cl}2}$ (5) also forms in 36% and 13% yields, respectively.

This coupling reaction of the copper(II) acetylide with incoming nucleophiles may be general. For instance, the reaction of $\text{Ph}-\text{Li}$ (1 equiv) with 3 (2 equiv) in cold THF afforded $\text{PhC}-\text{C}\equiv\text{C}\text{Ar}^{\text{Cl}2}$ (9) in 62% yield. Carrying out the reaction in a mixture of THF and benzene- d_6 , we observed the formation of both $[\text{Pr}_2\text{NN}]\text{Cu}(\text{benzene})$ and $\{[\text{Pr}_2\text{NN}]\text{Cu}-\text{C}\equiv\text{C}\text{Ar}^{\text{Cl}2}\}^-$ by ^1H NMR analysis (Figures 5d and S13). Considering the 2:1 $[\text{Pr}_2\text{NN}]\text{Cu}-\text{C}\equiv\text{C}\text{Ar}^{\text{Cl}2}:\text{Li}-\text{R}$ stoichiometry, a balanced reaction can be drawn (Figure 5d). This reactivity parallels the addition of a PhO^- nucleophile to the β -diketiminato-supported copper(II) aryl $[\text{Cu}^{\text{II}}]-\text{C}_6\text{F}_5$ (Figure 3) that results in the formation of the coupled organic product $\text{PhO}-\text{C}_6\text{F}_5$ along with a reduced copper species $[\text{Cu}^{\text{I}}](\text{solvent})$ and $\{[\text{Cu}^{\text{I}}]-\text{C}_6\text{F}_5\}^-$.²⁵

DFT studies support reaction pathways that proceed through redox disproportionation of the copper(II) acetylide into copper(III) and copper(I) acetylide complexes (Figure 6). In the absence of an added nucleophile, $[\text{Pr}_2\text{NN}]\text{Cu}^{\text{II}}-\text{C}\equiv\text{C}\text{Ar}^{\text{Cl}2}$ disproportionates to $\{[\text{Pr}_2\text{NN}]\text{Cu}^{\text{III}}-\text{C}\equiv\text{C}\text{Ar}^{\text{Cl}2}\}^+$ (8) and $\{[\text{Pr}_2\text{NN}]\text{Cu}^{\text{I}}-\text{C}\equiv\text{C}\text{Ar}^{\text{Cl}2}\}^-$ (4), facilitated by a polar solvent such as MeCN that stabilizes these charged species (Figure 6a). This accounts for the dramatic rate acceleration in MeCN vs benzene (Figure 5a). In the next step, anionic acetylide 4 attacks cationic acetylide 8 to form $[\text{Pr}_2\text{NN}]\text{Cu}^{\text{III}}(\text{C}\equiv\text{C}\text{Ar}^{\text{Cl}2})_2$ followed by reductive elimination that furnishes the homocoupled product $^{\text{Cl}2}\text{ArC}\equiv\text{C}-\text{C}\equiv\text{C}\text{Ar}^{\text{Cl}2}$ (5).

The addition of a nucleophile R^- stimulates redox disproportionation by stabilizing the higher oxidation state copper(III) intermediate. $[\text{Cu}^{\text{II}}]-\text{C}\equiv\text{C}\text{Ar}^{\text{Cl}2}$ (3) binds the nucleophile R^- , modeled as either $^{\text{Cl}2}\text{ArC}\equiv\text{C}^-$ or Ph^- , to form the four-coordinate $\{[\text{Cu}^{\text{II}}](\text{C}\equiv\text{C}\text{Ar}^{\text{Cl}2})\text{R}\}^-$ species (Figure 6b). Owing to their negative charge, electron-rich $\{[\text{Cu}^{\text{II}}](\text{C}\equiv\text{C}\text{Ar}^{\text{Cl}2})\text{R}\}^-$ complexes are especially unstable toward redox disproportionation in the presence of $[\text{Cu}^{\text{II}}]-\text{C}\equiv\text{C}\text{Ar}^{\text{Cl}2}$ (3) to give $[\text{Cu}^{\text{III}}](\text{C}\equiv\text{C}\text{Ar}^{\text{Cl}2})\text{R}$ along with the anionic acetylide $\{[\text{Cu}^{\text{I}}]-\text{C}\equiv\text{C}\text{Ar}^{\text{Cl}2}\}^-$ (4). Facile reductive elimination from $[\text{Cu}^{\text{III}}](\text{C}\equiv\text{C}\text{Ar}^{\text{Cl}2})\text{R}$ provides the corresponding C–C coupled products $\text{R}-\text{C}\equiv\text{C}\text{Ar}^{\text{Cl}2}$ (Figure 5b). As noted earlier, this mechanism is related to the Cu-mediated $\text{C}_{\text{sp}2}-\text{O}$ bond formation via a $[\text{Cu}^{\text{II}}]-\text{C}_6\text{F}_5$ intermediate (Figure 3b) that undergoes attack by a phenolate nucleophile PhO^- that triggers redox disproportionation between $\{[\text{Cu}^{\text{II}}](\text{C}_6\text{F}_5)-\text{OPh}\}^-$ and $[\text{Cu}^{\text{II}}]-\text{C}_6\text{F}_5$ to give $[\text{Cu}^{\text{III}}](\text{C}_6\text{F}_5)(\text{OPh})$, which rapidly reductively eliminates the diaryl ether $\text{PhO}-\text{C}_6\text{F}_5$.²⁵

$\text{C}_{\text{sp}}-\text{C}_{\text{sp}3}$ Coupling Mediated by $[\text{Pr}_2\text{NN}]\text{Cu}-\text{C}\equiv\text{C}\text{Ar}^{\text{Cl}2}$ (3) and Catalytic C–H Alkynylation. The copper(II) alkynyl $[\text{Pr}_2\text{NN}]\text{Cu}-\text{C}\equiv\text{C}\text{Ar}^{\text{Cl}2}$ (3) captures the radical $\text{Ph}_3\text{C}\cdot$ (formed in the equilibrium dissociation of Gomberg's dimer $\{\text{Ph}_3\text{C}\}_2$)³³ to form $\text{Ph}_3\text{C}-\text{C}\equiv\text{C}\text{Ar}^{\text{Cl}2}$ (10) within 5 min at RT in 69% yield along with $[\text{Pr}_2\text{NN}]\text{Cu}(\text{C}_6\text{D}_6)$ in 78% yield (Figure 7a). Because capture of radicals $\text{R}\cdot$ by $[\text{Cu}^{\text{II}}]-\text{FG}$ (FG = amide, anilide, alkoxides, phenoxide) to give $\text{R}-\text{FG}$ is the key C–FG bond-forming step in radical relay mechanisms for $\text{C}_{\text{sp}3}-\text{H}$ functionalization (Figure 7b, step (iv)),^{27,29,31,32,34–36} we explored the possibility of $\text{C}_{\text{sp}3}-\text{H}$ alkynylation mediated by copper(II) alkynyls $[\text{Cu}^{\text{II}}]-\text{C}\equiv\text{C}\text{R}$

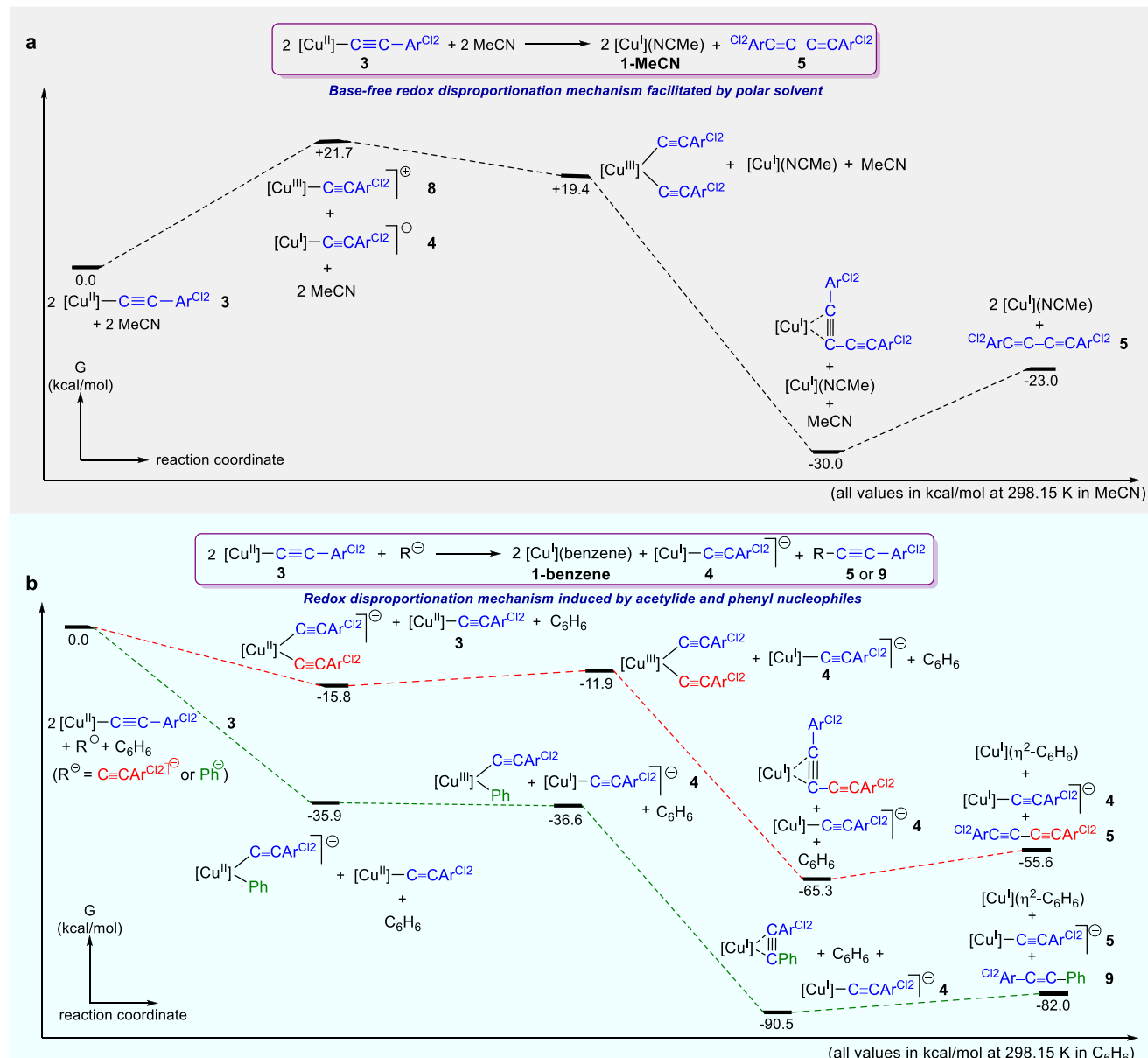


Figure 6. (a) DFT-calculated thermodynamic values for $\text{C}_{\text{sp}}-\text{C}_{\text{sp}}$ via redox disproportionation in polar solvents such as MeCN. (b) $\text{C}_{\text{sp}}-\text{C}_{\text{sp}}$ and $\text{C}_{\text{sp}}-\text{C}_{\text{sp}2}$ coupling reactions mediated by **3** that involve redox disproportionation/nucleophile transmetalation pathways. All computed free energies are reported at the BP86+GD₃B_J/6-311++G(d,p)/SMD-acetonitrile//BP68/6-311+G(d)/gas level of theory in kcal/mol at 25 °C.

generated by acid–base reaction of terminal alkynes $\text{H}-\text{C}\equiv\text{CR}$ with $[\text{Cu}^{\text{II}}]-\text{O}^{\text{-}}\text{Bu}$ intermediates readily formed upon reaction of β -diketiminato catalysts $[\text{Cu}^{\text{I}}]$ with $^{\text{t}}\text{BuOO}^{\text{-}}\text{Bu}$ (Figure 4b).³²

We embarked on catalytic $\text{C}_{\text{sp}}-\text{C}_{\text{sp}3}$ coupling^{11–13,19} by examining a model reaction of ethylbenzene (PhCH_2Me) with $\text{H}-\text{C}\equiv\text{C}\text{Ar}^{\text{CF}3}$ ($\text{Ar}^{\text{CF}3} = 4\text{-CF}_3\text{-C}_6\text{H}_4$) to form $\text{PhCH}(\text{C}\equiv\text{C}\text{Ar}^{\text{CF}3})\text{Me}$ under various conditions (Tables S3–S6). Several types of $\text{Cu}(\text{I})$ β -diketiminato catalysts were extensively screened in combination with various catalyst loadings, different oxidants, and different solvents (Tables S3–S6). The desired $\text{C}-\text{H}$ alkynylation product $\text{PhCH}(\text{C}\equiv\text{C}\text{Ar}^{\text{CF}3})\text{Me}$ forms along with $\text{CF}3\text{ArC}\equiv\text{C}-\text{C}\equiv\text{C}\text{Ar}^{\text{CF}3}$ and an alkene byproduct (Table S3).³⁷ While the $[\text{Pr}_2\text{NN}]\text{Cu}(\text{NCMe})$ (**1-MeCN**) catalyst provides a moderate yield of $\text{PhCH}(\text{C}\equiv\text{C}\text{Ar}^{\text{CF}3})\text{Me}$, the closely related $[\text{Cl}_2\text{NN}]\text{Cu}$ catalyst enhances

the $\text{C}_{\text{sp}3}-\text{H}$ alkynylation yield, especially when the catalyst loading is reduced from 5% to 1%, which effectively suppresses the Glaser homocoupled product $\text{CF}3\text{ArC}\equiv\text{C}-\text{C}\equiv\text{C}\text{Ar}^{\text{CF}3}$ (Table S4).

We next surveyed a range of $\text{C}_{\text{sp}3}-\text{H}$ substrates that undergo $\text{C}-\text{H}$ alkynylation with 1-chloro-2-ethynylbenzene (**11**). While a range of alkylbenzenes with benzylic $\text{C}-\text{H}$ bonds provide good yields (Table 1), we observed little success with substrates that possess only stronger, unactivated $\text{C}_{\text{sp}3}-\text{H}$ bonds such as cyclohexane or linear alkanes. Slower generation of R^{\cdot} radicals anticipated from stronger $\text{C}_{\text{sp}3}-\text{H}$ bonds in substrates $\text{R}-\text{H}$ may allow $\text{ArC}\equiv\text{C}-\text{C}\equiv\text{C}\text{Ar}$ formation from $[\text{Cu}^{\text{II}}]-\text{C}\equiv\text{C}\text{Ar}$ intermediates to compete with radical capture by R^{\cdot} to give the desired $\text{C}-\text{H}$ alkynylation products $\text{R}-\text{C}\equiv\text{C}\text{Ar}$.

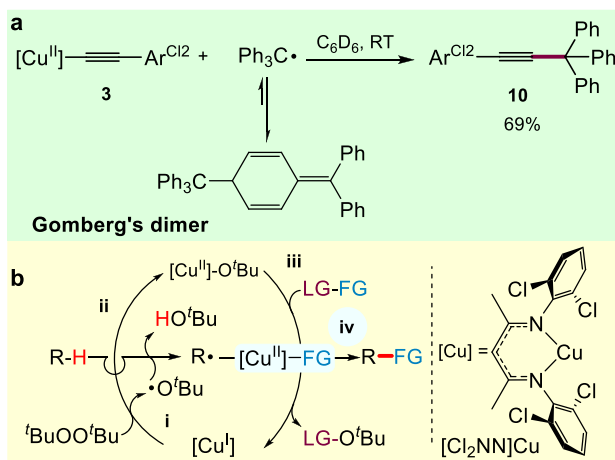
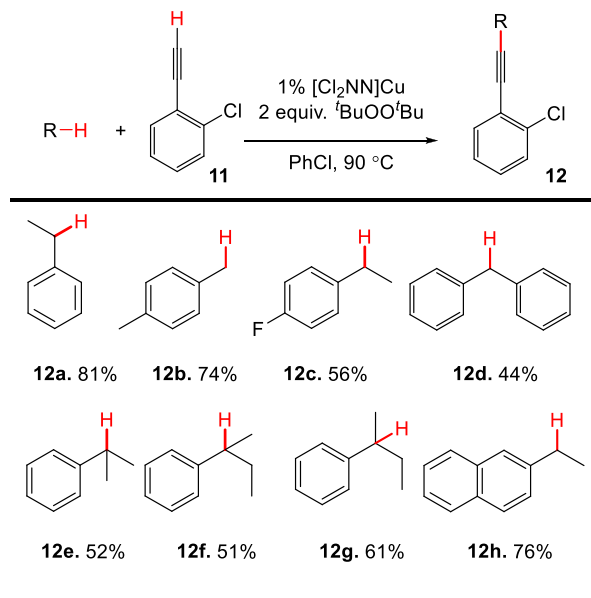


Figure 7. (a) Capture of the trityl radical $\text{Ph}_3\text{C}\cdot$ (via Gomberg's dimer) by 3 to form $\text{Ph}_3\text{C}-\text{C}\equiv\text{CAr}^{\text{Cl}2}$ (10). (b) Radical relay mechanism for catalytic C–N, C–O, and C–C bond formation.

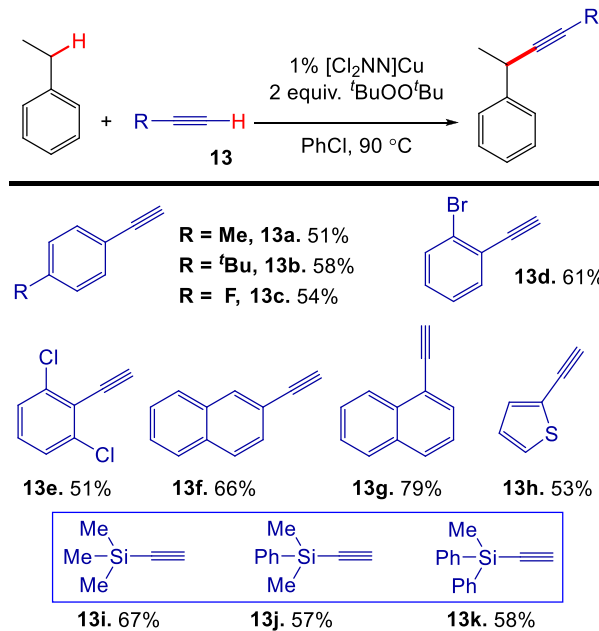
Table 1. Substrate Scope for Alkylation of 1-Chloro-2-ethynylbenzene Catalyzed by $[\text{Cl}_2\text{NN}]^{\text{Cu}}$ ^a



^aConditions: 0.5 equiv of 1-chloro-2-ethynylbenzene, 10 equiv of ethylbenzene, 2 equiv of ${}^{\text{t}}\text{BuOO}'\text{Bu}$, 90 °C in PhCl, 24 h. Isolated yields.

A range of terminal alkynes participate in the $\text{C}_{\text{sp}3}-\text{H}$ alkynylation of ethylbenzene (Table 2). Commercially available electron-rich (13a–13b) or electron-poor (13c–13e) aryl alkynes afforded good yields (51–66%). 1- and 2-Ethynylnaphthalene also participate in this $\text{C}_{\text{sp}3}-\text{H}$ alkynylation methodology to give the corresponding alkylated products 13g and 13f in 79% and 66% isolated yields, respectively. Gratifyingly, this methodology could also be applied in the alkylation of silyl-protected alkynes (13h–13j). For instance, the use of $\text{TMS}-\text{C}\equiv\text{CH}$ ($\text{TMS} = \text{SiMe}_3$) affords trimethyl(3-phenylbut-1-yn-1-yl)silane (13h) in 65% yield. Silyl-protected alkyne products $\text{R}'-\text{C}\equiv\text{C}-\text{SiR}_3$ are broadly useful as they can be directly deployed in cross-coupling reactions or easily deprotected to synthetically versatile terminal alkynes $\text{R}'-\text{C}\equiv\text{CH}$.

Table 2. C–H Alkynylation of Ethylbenzene with Various Terminal Alkynes, Including Silyl-Protected Alkynes 13h–13j^a



^aConditions: 0.5 equiv of terminal alkyne, 10 equiv of ethylbenzene, 2 equiv of ${}^{\text{t}}\text{BuOO}'\text{Bu}$, 90 °C in PhCl, 24 h. Isolated yields.

CONCLUSIONS

$[\text{Pr}_2\text{NN}]^{\text{Cu}}-\text{C}\equiv\text{CAr}^{\text{Cl}2}$ (3) represents the first crystallographically characterized mononuclear copper(II) alkynyl complex, representing a key intermediate in the valuable $\text{C}_{\text{sp}3}-\text{C}_{\text{sp}3}$ Glaser coupling reaction. Mechanistic studies reveal that such coupling is assisted by polar solvents such as MeCN, supporting a redox disproportionation pathway via charged $\{[\text{Cu}^{\text{III}}]-\text{C}\equiv\text{CR}\}^+$ and $\{[\text{Cu}^{\text{I}}]-\text{C}\equiv\text{CR}\}^-$ intermediates. Furthermore, the addition of 1/2 equiv of nucleophiles R' such as $\text{ArC}\equiv\text{C}-\text{Li}$ or $\text{Ph}-\text{Li}$ to $[\text{Pr}_2\text{NN}]^{\text{Cu}}-\text{C}\equiv\text{CAr}^{\text{Cl}2}$ results in the immediate formation of ${}^{\text{Cl}2}\text{ArC}\equiv\text{C}-\text{R}'$ with concomitant reduction to $\text{Cu}(\text{I})$ as both $[\text{Cu}^{\text{I}}](\text{solvent})$ and the $\text{Cu}(\text{I})$ alkynylate $\{[\text{Cu}^{\text{I}}]-\text{C}\equiv\text{CAr}^{\text{Cl}2}\}^-$. These observations shed light on other $\text{C}_{\text{sp}3}-\text{C}_{\text{sp}2}$ bond-forming reactions such as the Pd-free Sonogashira reactions.^{8,20,21} Additionally, $[\text{Cu}^{\text{II}}]-\text{C}\equiv\text{CAr}^{\text{Cl}2}$ cleanly reacts with Gomberg's dimer to provide $\text{Ph}_3\text{C}-\text{C}\equiv\text{CAr}^{\text{Cl}2}$ (10), indicating the ability of $[\text{Cu}^{\text{II}}]-\text{C}\equiv\text{CAr}^{\text{Cl}2}$ to capture alkyl radicals $\cdot\text{R}'$. On the basis of this key finding, we developed a Cu-catalyzed C–H alkynylation protocol featuring Cu(II) alkynyls.

This report underscores the diverse roles that copper(II) organometallic intermediates play in cross coupling and C–H functionalization catalysis. Such $[\text{Cu}^{\text{II}}]-\text{R}'$ ($\text{R}' = \text{aryl}$ or alkyne) species undergo homocoupling reactions to form new $\text{C}_{\text{sp}2}-\text{C}_{\text{sp}2}$ or $\text{C}_{\text{sp}}-\text{C}_{\text{sp}}$ bonds in $\text{R}'-\text{R}'$ homocoupling products connected to the Ullman ($\text{R}' = \text{aryl}$)³⁹ or Glaser ($\text{R}' = \text{alkynyl}$) couplings (Figure 8a).⁴⁰ Importantly, these $\text{R}'-\text{R}'$ bond-forming reactions do not appear to be simple bimolecular couplings of $[\text{Cu}^{\text{II}}]-\text{R}'$ intermediates. Rather, they proceed via redox disproportionation to $\{[\text{Cu}^{\text{III}}]-\text{R}'\}^+$ and $\{[\text{Cu}^{\text{I}}]-\text{R}'\}^-$ species that can generate $[\text{Cu}^{\text{III}}](\text{R}')_2$ intermediates that are susceptible to facile reductive elimination of $\text{R}'-\text{R}'$. Addition of a nucleophile Nu^- to such $[\text{Cu}^{\text{II}}]-\text{R}'$ species stimulates this redox disproportionation by facilitating the formation of more

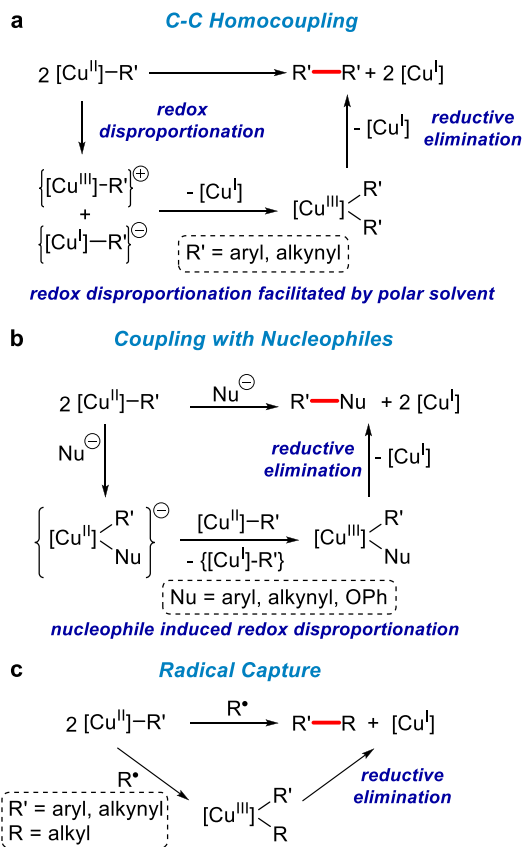


Figure 8. Organocopper(II) intermediates in (a) Ullman- or Glaser-type homocoupling reactions, (b) C–C and C–O bond formation with nucleophiles, and (c) C–C bond formation via the capture of alkyl radicals.

electron-rich $[\text{Cu}^{\text{III}}](\text{R}')(\text{Nu})$ species that reductively eliminate $\text{Nu}-\text{R}'$ products (Figure 8b). On the other hand, the addition of a Lewis base that is resistant to cross-coupling L to copper(II) alkynyl 3 such as the pyridine derivative 2,4-lutidine accelerates homocoupling, perhaps by stabilizing cationic copper(III) intermediates $\{[\text{Cu}^{\text{III}}](\text{R})(\text{L})\}^+$. The addition of a nucleophile Nu^- that can engage in cross-coupling, however, is connected to the Chan–Lam–Evans coupling that commonly employs boronate esters $(\text{R}''\text{O})_2\text{B}-\text{R}'$ with O- and N-based nucleophiles under copper catalysis.^{41,42} Lastly, such $[\text{Cu}^{\text{II}}]-\text{R}'$ species are rather reactive toward incoming radicals R^\bullet generated under catalytic C–H functionalization conditions employed in radical relay catalysis. $\text{R}-\text{R}'$ coupled products form, perhaps via $[\text{Cu}^{\text{III}}](\text{R})(\text{R}')$ intermediates that are unstable toward reductive elimination (Figure 8c).⁴³ Copper(II) organometallic species $[\text{Cu}^{\text{II}}]-\text{R}'$ thus enable facile coupling of C–C_{sp}, C–C_{sp2}, and C–C_{sp3} bonds.

ASSOCIATED CONTENT

Supporting Information

The Supporting Information is available free of charge at <https://pubs.acs.org/doi/10.1021/jacs.0c07137>.

General instrumentation and physical methods, materials, synthesis and characterization data, crystallographic details and additional structures, references for synthetic and crystallographic details, computational details, and spectral data (PDF)

X-ray crystallographic data for 2 (CIF)

X-ray crystallographic data for 3 (CIF)
X-ray crystallographic data for 10 (CIF)

AUTHOR INFORMATION

Corresponding Author

Timothy H. Warren — Department of Chemistry, Georgetown University, Washington, District of Columbia 20057, United States; orcid.org/0000-0001-9217-8890; Email: thw@georgetown.edu

Authors

Abolghasem Bakhoda — Department of Chemistry, Georgetown University, Washington, District of Columbia 20057, United States; orcid.org/0000-0002-3222-8873

Otome E. Okoromoba — Department of Chemistry, Georgetown University, Washington, District of Columbia 20057, United States; orcid.org/0000-0001-8963-8390

Christine Greene — Department of Chemistry, Georgetown University, Washington, District of Columbia 20057, United States

Mahdi Raghibi Boroujeni — Department of Chemistry, Georgetown University, Washington, District of Columbia 20057, United States; orcid.org/0000-0001-8146-5878

Jeffery A. Bertke — Department of Chemistry, Georgetown University, Washington, District of Columbia 20057, United States; orcid.org/0000-0002-3419-5163

Complete contact information is available at: <https://pubs.acs.org/10.1021/jacs.0c07137>

Author Contributions

[‡]A.B. and O.E.O. contributed equally.

Notes

The authors declare no competing financial interest.

The X-ray crystallographic data for 2, 3, and 10 have been deposited at the Cambridge Crystallographic Data Centre (CCDC) under deposition number CCDC 1938189–1938191, respectively. These data can be obtained free of charge from The Cambridge Crystallographic Data Centre (www.ccdc.cam.ac.uk/data_request/cif).

ACKNOWLEDGMENTS

We are grateful for support by the U.S. National Science Foundation (CHE-1665348) and the Georgetown Environment Initiative (T.H.W.).

REFERENCES

- (1) Knochel, P.; Molander, G. A. *Comprehensive Organic Synthesis*, 2nd ed.; Elsevier: Amsterdam, The Netherlands, 2014.
- (2) Glaser, C. Beiträge zur Kenntnis des Acetenylbenzols. *Ber. Dtsch. Chem. Ges.* **1869**, 2, 422–424.
- (3) Salkind, J. S.; Fundyler, F. B. A New Synthesis of Diacetylenederivative. *Ber. Dtsch. Chem. Ges. B* **1936**, 69, 128–130.
- (4) Bohlmann, F.; Schönowsky, H.; Inhoffen, E.; Grau, G. Polyacetylenverbindungen, LII. Über den Mechanismus der Öxidativen Dimerisierung von Acetylenverbindungen. *Chem. Ber.* **1964**, 97, 794–800.
- (5) Vilhelmsen, M. H.; Jensen, J.; Tortzen, C. G.; Nielsen, M. B. The Glaser-Hay Reaction: Optimization and Scope Based on ¹³C NMR Kinetics Experiments. *Eur. J. Org. Chem.* **2013**, 2013, 701–711.
- (6) Hay, A. S. Oxidative Coupling of Acetylenes. II. *J. Org. Chem.* **1962**, 27, 3320–3321.
- (7) Van Koten, G.; James, S. L.; Jastrzebski, J. T. B. H. Copper and Silver. *Comprehensive Organometallic Chemistry II*. **1995**, 57–133.

(8) Dong, X.-Y.; Zhang, Y.-F.; Ma, C.-L.; Gu, Q.-S.; Wang, F.-L.; Li, Z.-L.; Jiang, S.-P.; Liu, X.-Y. A General Asymmetric Copper-Catalyzed Sonogashira C(sp₃)-C(sp) Coupling. *Nat. Chem.* **2019**, *11*, 1158–1166.

(9) Fu, L.; Zhou, S.; Wan, X.; Chen, P.; Liu, G. Enantioselective Trifluoromethylalkynylation of Alkenes via Copper-Catalyzed Radical Relay. *J. Am. Chem. Soc.* **2018**, *140*, 10965–10969.

(10) Zhu, L.; Brassard, C. J.; Zhang, X.; Guha, P. M.; Clark, R. J. On the Mechanism of Copper(I)-Catalyzed Azide-Alkyne Cycloaddition. *Chem. Rec.* **2016**, *16*, 1501–1517.

(11) Tang, S.; Liu, Y.; Gao, X.; Wang, P.; Huang, P.; Lei, A. Multi-Metal-Catalyzed Oxidative Radical Alkynylation with Terminal Alkynes: A New Strategy for C(sp₃)-C(sp) Bond Formation. *J. Am. Chem. Soc.* **2018**, *140*, 6006–6013.

(12) Tang, S.; Wang, P.; Li, H.; Lei, A. Multimetallic Catalysed Radical Oxidative C(sp₃)-H/C(sp)-H Cross-Coupling Between Unactivated Alkanes and Terminal Alkynes. *Nat. Commun.* **2016**, *7*, 11676.

(13) Zhang, Z.-H.; Dong, X.-Y.; Du, X.-Y.; Gu, Q.-S.; Li, Z.-L.; Liu, X.-Y. Copper-Catalyzed Enantioselective Sonogashira-Type Oxidative Cross-Coupling of Unactivated C(sp₃)-H Bonds with Alkynes. *Nat. Commun.* **2019**, *10*, 5689.

(14) Zhang, G.; Yi, H.; Zhang, G.; Deng, Y.; Bai, R.; Zhang, H.; Miller, J. T.; Kropf, A. J.; Bunel, E. E.; Lei, A. Direct Observation of Reduction of Cu(II) to Cu(I) by Terminal Alkynes. *J. Am. Chem. Soc.* **2014**, *136*, 924–926.

(15) Bai, R.; Zhang, G.; Yi, H.; Huang, Z.; Qi, X.; Liu, C.; Miller, J. T.; Kropf, A. J.; Bunel, E. E.; Lan, Y.; Lei, A. Cu(II)-Cu(I) Synergistic Cooperation to Lead the Alkyne C-H Activation. *J. Am. Chem. Soc.* **2014**, *136*, 16760–16763.

(16) Feng, L.; Hu, T.; Zhang, S.; Xiong, H.-Y.; Zhang, G. Copper-Mediated Deacylative Coupling of Ynones via C-C Bond Activation under Mild Conditions. *Org. Lett.* **2019**, *21*, 9487–9492.

(17) Hamada, T.; Ye, X.; Stahl, S. S. Copper-Catalyzed Aerobic Oxidative Amidation of Terminal Alkynes: Efficient Synthesis of Ynamides. *J. Am. Chem. Soc.* **2008**, *130*, 833–835.

(18) Wang, L.; Huang, H.; Priebbenow, D. L.; Pan, F.-F.; Bolm, C. Copper-Catalyzed Oxidative Cross-Coupling of Sulfoximines and Alkynes. *Angew. Chem., Int. Ed.* **2013**, *52*, 3478–3480.

(19) Fu, L.; Zhang, Z.; Chen, P.; Lin, Z.; Liu, G. Enantioselective Copper-Catalyzed Alkynylation of Benzylic C-H Bonds via Radical Relay. *J. Am. Chem. Soc.* **2020**, *142*, 12493–12500.

(20) Hazra, A.; Lee, T. M.; Chiu, J. F.; Lalic, G. Photoinduced Copper-Catalyzed Coupling of Terminal Alkynes and Alkyl Iodides. *Angew. Chem., Int. Ed.* **2018**, *57*, 5492–5496.

(21) Cao, Y.-X.; Dong, X.-Y.; Yang, J.; Jiang, S.-P.; Zhou, S.; Li, Z.-L.; Chen, G.-Q.; Liu, X.-Y. A Copper-Catalyzed Sonogashira Coupling Reaction of Diverse Activated Alkyl Halides with Terminal Alkynes Under Ambient Conditions. *Adv. Synth. Catal.* **2020**, *362*, 2280–2284.

(22) Lang, H.; Jakob, A.; Milde, B. Copper(I) Alkyne and Alkynide Complexes. *Organometallics* **2012**, *31*, 7661–7693.

(23) Zhang, Q.; Wang, T.; Zhang, X.; Tong, S.; Wu, Y.-D.; Wang, M.-X. Radical Reactivity, Catalysis, and Reaction Mechanism of Arylcopper(II) Compounds: The Missing Link in Organocopper Chemistry. *J. Am. Chem. Soc.* **2019**, *141*, 18341–18348.

(24) Ziegler, M. S.; Lakshmi, K. V.; Tilley, T. D. Dicopper Cu(I)Cu(I) and Cu(I)Cu(II) Complexes in Copper-Catalyzed Azide-Alkyne Cycloaddition. *J. Am. Chem. Soc.* **2017**, *139*, 5378–5386.

(25) Kundu, S.; Greene, C.; Williams, K. D.; Salvador, T. K.; Bertke, J. A.; Cundari, T. R.; Warren, T. H. Three-Coordinate Copper(II) Aryls: Key Intermediates in C-O Bond Formation. *J. Am. Chem. Soc.* **2017**, *139*, 9112–9115.

(26) Bakhoda, A.; Jiang, Q.; Bertke, J. A.; Cundari, T. R.; Warren, T. H. Elusive Terminal Copper Arylnitrene Intermediates. *Angew. Chem., Int. Ed.* **2017**, *56*, 6426–6430.

(27) Wiese, S.; Badiei, Y. M.; Gephart, R. T.; Mossin, S.; Varonka, M. S.; Melzer, M. M.; Meyer, K.; Cundari, T. R.; Warren, T. H. C-H Amination with Unactivated Amines Through Copper(II) Amides. *Angew. Chem., Int. Ed.* **2010**, *49*, 8850–8855.

(28) Melzer, M. M.; Mossin, S.; Cardenas, A. J. P.; Williams, K. D.; Zhang, S.; Meyer, K.; Warren, T. H. A Copper(II) Thiolate from Reductive Cleavage of an S-Nitrosothiol. *Inorg. Chem.* **2012**, *51*, 8658–8660.

(29) Salvador, T. K.; Arnett, C. H.; Kundu, S. K.; Sapiezynski, N. G.; Bertke, J. A.; Raghibi Boroujeni, M.; Warren, T. H. Copper Catalyzed sp₃ C-H Etherification with Acyl Protected Phenols. *J. Am. Chem. Soc.* **2016**, *138*, 16580–16583.

(30) Melzer, M. M.; Mossin, S.; Dai, X.; Bartell, A. M.; Kapoor, P.; Meyer, K.; Warren, T. H. A Three-Coordinate Copper(II) Amide from Reductive Cleavage of a Nitrosamine. *Angew. Chem., Int. Ed.* **2010**, *49*, 904–907.

(31) Jang, E. S.; McMullin, C. L.; Käß, M.; Meyer, K.; Cundari, T. R.; Warren, T. H. Copper(II) Anilides in sp₃ C-H Amination. *J. Am. Chem. Soc.* **2014**, *136*, 10930–10940.

(32) Gephart, R. T.; McMullin, C. L.; Sapiezynski, N. G.; Jang, E. S.; Aguila, M. J.; Cundari, T. R.; Warren, T. H. Reaction of Cu(I) with Dialkyl Peroxides: Cu(II)-Alkoxides, Alkoxy Radicals, and Catalytic C-H Etherification. *J. Am. Chem. Soc.* **2012**, *134*, 17350–17353.

(33) Gomberg, M. The Existence of Free Radicals. *J. Am. Chem. Soc.* **1914**, *36*, 1144–1170.

(34) Gephart, R. T.; Huang, D. L.; Aguila, M. J.; Schmidt, G.; Shah, A.; Warren, T. H. Catalytic C-H Amination with Aromatic Amines. *Angew. Chem., Int. Ed.* **2012**, *51*, 6488–6492.

(35) Kharasch, M. S.; Sosnovsky, G. *J. Am. Chem. Soc.* **1958**, *80*, 756.

(36) Kharasch, M. S.; Sosnovsky, G.; Yang, N. C. *J. Am. Chem. Soc.* **1959**, *81* (21), 5819–5824.

(37) Song, Z.-Q.; Liu, Z.; Gan, Q.-C.; Lei, T.; Tung, C.-H.; Wu, L.-Z. Photoredox Oxo-C(sp₃)-H Bond Functionalization via in Situ Cu(I)-Acetylide Catalysis. *Org. Lett.* **2020**, *22*, 832–836.

(38) Porey, S.; Zhang, X.; Bhowmick, S.; Kumar Singh, V.; Guin, S.; Paton, R. S.; Maiti, D. Alkyne Linchpin Strategy for Drug-Pharmacophore Conjugation: Experimental and Computational Realization of a Meta-Selective Inverse Sonogashira Coupling. *J. Am. Chem. Soc.* **2020**, *142*, 3762–3774.

(39) Hassan, J.; Sévignon, M.; Gozzi, C.; Schulz, E.; Lemaire, M. Aryl-Aryl Bond Formation One Century after the Discovery of the Ullmann Reaction. *Chem. Rev.* **2002**, *102*, 1359–1469.

(40) Siemsen, P.; Livingston, R. C.; Diederich, F. Acetylenic Coupling: A Powerful Tool in Molecular Construction. *Angew. Chem., Int. Ed.* **2000**, *39*, 2632–2657.

(41) Vantourout, J. C.; Miras, H. N.; Isidro-Llobet, A.; Sproules, S.; Watson, A. J. B. Spectroscopic Studies of the Chan-Lam Amination: A Mechanism Inspired Solution to Boronic Ester Reactivity. *J. Am. Chem. Soc.* **2017**, *139*, 4769–4779.

(42) West, M. J.; Fyfe, J. W. B.; Vantourout, J. C.; Watson, A. J. B. Mechanistic Development and Recent Applications of the Chan-Lam Amination. *Chem. Rev.* **2019**, *119*, 12491–12523.

(43) On the basis of a recent spectroscopic/computational study by Lancaster and colleagues, such copper(III) complexes may not possess simple d⁸ configurations due to the high covalency of Cu–R bonds owing to the relatively high electronegativity of Cu: DiMucci, I. M.; Lukens, J. T.; Chatterjee, S.; Carsch, K. M.; Titus, C. J.; Lee, S. J.; Nordlund, D.; Betley, T. A.; MacMillan, S. N.; Lancaster, K. M. The Myth of d⁸ Copper(III). *J. Am. Chem. Soc.* **2019**, *141*, 18508–18520.